Journal of Chromatography A, 1218 (2011) 2460–2466

Contents lists available at ScienceDirect

Journal of Chromatography A

journal homepage: www.elsevier.com/locate/chroma

# Peak spreading in linear gradient elution chromatography with a thin monolithic disk

Shuichi Yamamoto*, Tomomi Okada, Mitsuyo Abe, Noriko Yoshimoto

*Bio-Process Engineering Laboratory, School of Engineering and Graduate School of Medicine, Yamaguchi University, Tokiwadai, Ube 755-8611, Japan*

ARTICLE INFO

*Article history:*
Available online 13 March 2011

*Keywords:*
Ion-exchange chromatography
Linear gradient elution
Peak width
Binding site
Monolith

ABSTRACT

The peak spreading of DNAs of various sizes [12-mer, 20-mer, 50-mer and 95-mer poly(T)] in linear gradient elution (LGE) chromatography with a thin monolithic disk was investigated by using our method developed for determining HETP in LGE. Electrostatic interaction-based chromatography mode (ion-exchange chromatography, IEC) was used. Polymer-based monolithic disks of two different sizes (12 mm diameter, 3 mm thickness and 0.34 mL; 5.2 mm diameter, 4.95 mm thickness and 0.105 mL) having anion-exchange groups were employed. For comparison, a 15-μm porous bead IEC column (Resource Q, 6.4 mm diameter, 30 mm height and 0.97 mL) was also used. The peak width did not change with the flow velocity for the monolithic disks where as it became wider with increasing velocity. For the monolithic disks the peak width normalized with the column bed volume was well-correlated with the distribution coefficient at the peak position $K_R$. HETP values were constant (ca. 0.003–0.005 cm) when $K_R > 5$. Much higher HETP values which are flow-rate dependent were obtained for the porous bead chromatography. It is possible to obtain 50–100 plates for the 3 mm monolithic disk. This results in very sharp elution peaks (standard deviation/bed volume = 0.15) even for stepwise elution chromatography, where the peak width is similar to that for LGE of a very steep gradient slope.



Although M (=mol/dm$^3$) is not a SI unit, it is used in this paper for the sake of convenience.

## 1. Introduction

It has been shown since late 80s that convection-controlled chromatography allows separation at high flow velocities (high-speed separation) [1–7]. However, for preparative and process scale separations the advantages of convection-aided chromatography are not clear as there are many constraints such as low pressure drops and large particle diameters of chromatography media.

Theoretically, the pressure drop across the chromatography packing particle causes the intra-particle convection (through pores) [1–7]. The key parameter is therefore, the ratio between the particle diameter to the effective through pore diameter, $d_p/d_{tp}$. Smaller $d_p$ and large $d_{tp}$ can enhance the intra-particle convection. However, smaller particles are not preferred for the process scale separations as the pressure drop increases and the cost of packing is high. Mechanical stability of particles basically decreases with increasing $d_{tp}$.

When large particles such as 90–100 μm are used, the flow velocity must be high enough so that the intra-particle convection occurs. In most cases such high flow velocities are unrealistic for process scale separations.

On the other hand, real convection-controlling chromatography, in which diffusive pores are almost negligible and most pores are convective flow-channels, is available as membrane chromatography or monolithic chromatography [8–20]. Several thin membranes such as 100 μm must be stacked for membrane chromatography in order to obtain reasonable thickness of the chromatography bed [8,9]. However, this causes additional problems such as mal-flow distribution or extra zone spreading. Monolith, by definition, is a continuous phase chromatography so that the bed is uniform and the flow channels are continuous like the inter-particle space of the packed bed bead chromatography [13–20].

Currently, most membrane-based chromatography or adsorber is aimed for single-use flow-through chromatography applications such as removal of DNAs and host cell proteins (HCPs) [11,12]. Eventually, desorption (elution) is not considered important.

On the other hand, as shown previously monolith chromatography is best suited for purification of large biomolecules or bioparticles such as Immunoglobulins, plasmid DNAs and

* Corresponding author. Tel.: +81 836 85 9241; fax: +81 836 85 9201.
*E-mail address:* shuichi@yamaguchi-u.ac.jp (S. Yamamoto).

0021-9673/$ – see front matter © 2011 Elsevier B.V. All rights reserved.
doi:10.1016/j.chroma.2011.03.013

**Nomenclature**

| | |
|---|---|
| $A$ | $K_e \Lambda^B$ |
| $A_c$ | cross-sectional area [$cm^2$] |
| $A^0$ | first term in Eq. (14) [cm] |
| $B$ | the number of binding sites |
| $B^0$ | second term in Eq. (14) [$m^2$/s] |
| $C_0$ | initial concentration [mg/mL] |
| $C^0$ | third term in Eq. (14) [s or min] |
| $D_L$ | axial dispersion coefficient [$m^2$/s] |
| $D_s$ | stationary phase diffusion coefficient [$m^2$/s] |
| $D^0$ | fourth term in Eq. (14) [s or min] |
| $d_p$ | particle diameter [cm] |
| $F$ | volumetric flow rate [mL/min] |
| $G$ | normalized gradient slope = $(g V_0)$ [M] |
| $g$ | gradient slope = $(I_f - I_0)/V_g = (I_f - I_0)/(Ft_g)$ [M/mL] |
| $GH$ | normalized gradient slope = $(g V_0)H = g(V_t - V_0)$ [M] |
| $H$ | phase ratio = $(V_t - V_0)/V_0 = (1 - \varepsilon)/\varepsilon$ |
| HETP | Plate height, Height equivalent to a theoretical plate [cm] |
| $I$ | salt concentration [M] |
| $I_f$ | final salt concentration [M] |
| $I_0$ | initial salt concentration [M] |
| $I_R$ | peak salt concentration [M] |
| $J$ | absolute value of $dK/dI$ at $I = I_R$ [$M^{-1}$] |
| $K$ | distribution coefficient |
| $K'$ | distribution coefficient of salt |
| $K_e$ | equilibrium association constant |
| $K_R$ | $K$ at $I = I_R$ |
| $k_F$ | film mass transfer coefficient [m/s] |
| $L$ | zone spreading factor defined by Eq. (9) |
| $M$ | dimensionless variable defined by Eq. (10) |
| $t_g$ | gradient time [min] |
| $t_R$ | retention time [min] |
| $u$ | linear mobile phase velocity = $F/(A_c\varepsilon)$ [cm/min] |
| $V$ | elution volume [mL] |
| $V'$ | elution volume for the salt [mL] |
| $V_g$ | gradient volume [mL] |
| $V_0$ | column void volume (interstitial volume) [mL] |
| $V_R$ | retention volume [mL] |
| $V_t$ | column volume [mL] |
| $W$ | peak width at the base line [min] |
| $W_V$ | peak width at the base line [mL] |
| $w$ | peak width measured at 0.368 × peak height [min] |
| $w_V$ | peak width measured at 0.368 × peak height [mL] |
| $\varepsilon$ | void fraction of column = $V_0/V_t$ |
| $\Lambda$ | total ion exchange capacity [mequiv/mL] |
| $\sigma$ | standard deviation of the peak [min] |
| $\sigma_v$ | standard deviation of the peak [mL] |

vaccines [19]. For these applications both adsorption and desorption performance must be high and well-understood. We have analysed the zone spreading behavior in linear gradient elution (LGE) ion exchange chromatography (IEC) of oligo-DNAs and reported that the oligo DNA peak is quite narrow due to the large binding site and the zone sharpening effect [20].

The purpose of this paper is therefore to understand the zone spreading in a short-monolithic layer or disk during elution. Several studies were reported on the zone spreading in monolithic chromatography mainly by using isocratic elution (or pulse response method) under non-tight binding conditions [13,15–18]. However, the data in LGE (under tight binding and elution conditions) have not yet been fully analysed. The method for measuring HETP from linear gradient elution (LGE) curves [21] was applied to the data with monolithic disks as well as conventional porous bead chromatography. As a comparison, the data with conventional porous 15 μm particle bead packed bed chromatography was also analysed. The model samples were DNAs of different sizes and electrostatic-interaction based chromatography mode (ion-exchange chromatography, IEC) was used.

## 2. Experimental

The method and equipment are essentially the same as those in our previous study [22].

### 2.1. Chromatography column

Poly(glycidyl methacrylate-co-ethylene dimethacrylate) disks (12 mm diameter × 3 mm thickness, total volume $V_t$ = 0.34 mL) with strong anion exchange group (QA) were contained in a specially designed disk holder column from BIA Separations (Ljubljana, Slovenia). This disk is called hereafter CIM std. A smaller unit (5.2 mm diameter × 4.95 mm thickness, $V_t$ = 0.105 mL) from the same supplier was also employed (hereafter, it is called CIM mini).

As a comparison a porous-15 μm particle strong anion exchange chromatography column (Resource Q, 6.4 mm diameter × 30 mm, $V_t$ = 0.965 mL GE-Healthcare, Uppsala, Sweden) was employed.

### 2.2. Materials

Oligonucelotides (DNAs) 12-mer poly (T), 20-mer poly (T), 50-mer poly (T) and 95-mer poly (T) (purified by C18 HPLC) were purchased from Tsukuba Oligo Service (Tsukuba, Japan). The supplier attached the chromatogram by C18 HPLC for each product. Prior to use for chromatography oligonucleotide samples were thermally pretreated according to the following temperature program: from 25 °C to 95 °C (20 min), 95 °C (3 min), from 95 °C to 40 °C (20 min) and from 40 °C to 25 °C (45 min). We also tested the following simple pretreatment method. The sample solution was placed in a boiling water bath for 5 min and then cooled on ice. The elution curves by the two methods were superimposable. Without pretreatments small peaks were observed as well as the main peak. These small peaks may be due to aggregation. When the sample solution stored in a freezer was used, very small peaks and small tailing were sometimes observed. Therefore, the sample was freshly prepared and thermally pretreated before experiments. Other reagents were of analytical grade.

### 2.3. Chromatography setup

Chromatography experiments were carried out on a fully automated liquid chromatography system ÄKTA Explorer 10S (GE Health Care, Uppsala, Sweden). As ÄKTA system is not designed for a small high performance column, the dead volume is relatively large. The dead volume due to the connection tubes was reduced as much as possible. The CIM disk holder was directly connected to the UV cell (UV-cell volume 0.008 mL). As for the inlet line, the tube between the disk holder inlet and the injection valve was connected with a short and narrow tube (tube diameter 0.5 mm, volume 0.07 mL).

### 2.4. Linear gradient elution experiment

The column was equilibrated with a starting buffer (buffer A) containing a specified concentration of NaCl (in most cases 0.2 M).

The same buffer solution containing 0.5–2.0 M NaCl was used as a final elution buffer (buffer B). The linear gradient elution was performed by changing the buffer composition linearly from buffer A to buffer B with time. Namely, the NaCl concentration was increased with time at a fixed pH and buffer compositions. The gradient slope $g$ is shown in M/mL. The linear mobile phase velocity $u$ was calculated with the cross-sectional area $A_c$ and the column bed void fraction $\varepsilon$ as $u = F/(A_c \cdot \varepsilon)$ where $F$ is the volumetric flow rate. The column bed void fraction $\varepsilon$ was determined from the peak retention volume of Dextran T 2000 pulses. For the CIM disks, the void fraction was assumed to be 0.60 [13,14]. The experiments were performed at 25 ± 1 °C. We examined the effect of pH by using different buffer A solutions, and found the peak retention volume does not change in the range of pH 7–9. In this study 14 mM Tris–HCl (pH 7.7) was chosen as buffer A. Unless otherwise noted, the volumetric flow-rate $F$ was from 0.5 to 3.0 $cm^3$/min for Resource Q, 1.0–2.0 $cm^3$/min for CIM std and 0.28, 0.5 and 1.0 $cm^3$/min for CIM mini. The sample injection volume was 0.01 $cm^3$. Experiments were carried out for at least four different gradient slopes. Each run was at least repeated twice.

## 3. Theoretical

### 3.1. A and B parameter determination from linear gradient elution curve

The outline of our model for determining the two parameters $A$ and $B$ [19–24] from linear gradient elution (LGE) experimental data is briefly explained below. The peak retention volume is a function of gradient slope in LGE–IEC. The peak salt concentration $I_R$ increases with increasing gradient slope. The $I_R$ values can be correlated with the following normalized gradient slope,

$$GH = (gV_0)\left[\frac{V_t - V_0}{V_0}\right] = g(V_t - V_0) \quad (1)$$

$V_t$ is the total bed volume, $V_0$ is the column void volume (interstitial volume of the bed), and $g$ is the gradient slope of the salt. $H = (V_t - V_0)/V = (1-\varepsilon)/\varepsilon$ is the phase ratio. $\varepsilon = V_0/V_t$ is the bed void fraction. The gradient slope $g$ is defined by the following equation.

$$g = \frac{I_f - I_0}{V_g} = \frac{I_f - I_0}{Ft_g} \quad (2)$$

$I_f$ is the final salt concentration, $I_0$ is the initial salt concentration, $V_g$ is the gradient volume, $F$ is the volumetric flow rate, and $t_g$ is the gradient time. Linear gradient elution experiments are performed at different gradient slopes ($GH$ values) at a fixed pH. The salt concentration at the peak position $I_R$ is determined as a function of $GH$. The $GH$–$I_R$ curves thus constructed do not depend on the flow velocity, the column dimension, the sample loading (if the overloading condition is not used), or the initial salt concentration $I_0$ [19–24]. The experimental $GH$–$I_R$ data can commonly be expressed by the following equation [19–24].

$$GH = \frac{I_R^{B+1}}{A(B+1)} \quad (3)$$

From the law of mass action (ion exchange equilibrium or stochastic displacement model) [23–29], the following relationship can be derived.

$$A = K_e \Lambda^B \quad (4)$$

here, $B$ is the number of sites (effective charges) involved in electrostatic interaction, which is basically the same as the $Z$ number [25,26] and the characteristic charge [27,28], $K_e$ is the equilibrium association constant, and $\Lambda$ is the total ion exchange capacity. From the ion-exchange equilibrium model and Eq. (4), the following equation is derived [19–24].

$$K - K' = K_e \Lambda^B I^{-B} \quad (5)$$

here $K$ is the protein distribution coefficient, $K'$ is the distribution coefficient of salt, and $I$ is the salt concentration (counter ion concentration). The SMA model equation [27,28] is reduced to Eq. (5) when the sample loading is low ($\Lambda$ is not affected by sample adsorption). More detailed analysis on multivalent interaction in chromatography has been reported by Velayudan and Horvath [29].

### 3.2. HETP determination from linear gradient elution curve

The conventional method for determining HETP (a height equivalent to a theoretical plate) cannot be applied directly to linear gradient elution. We therefore developed a method for determining HETP from linear gradient elution curves [21]. A similar method, which was developed based on a different concept has been proposed by Snyder [30]. These two methods are explained in [31].

The usual definition of HETP (isocratic elution at constant $K$) is

$$HETP = \frac{Z}{N} = Z\left(\frac{\sigma}{t_R}\right)^2 = Z\frac{(w/t_R)^2}{8} = Z\frac{(W/t_R)^2}{16} = Z\left(\frac{\sigma_V}{V_R}\right)^2 = Z\frac{(w_V/V_R)^2}{8} = Z\frac{(W_V/V_R)^2}{16} \quad (6)$$

The subscript $V$ implies the volume based value.The elution volume $V_R$ can be related to the distribution coefficient $K$ and the phase ratio $H$.

$$V_R = V_0(1 + HK_R) \quad (7)$$

The plate number $N$ is given by

$$N = \left(\frac{V_R}{\sigma_v}\right)^2 = \left[\frac{V_0(1+HK_R)}{\sigma_V}\right]^2 \quad (8)$$

In isocratic elution $K_R$ is constant. However, in linear gradient elution it changes with time or elution volume. In addition, the zone sharpening effect makes the peak narrower.

The degree of zone sharpening effect defined as $L$ is correlated with the dimensionless variable $M$.

$$L = \frac{W(\text{gradient elution})}{W(\text{isocratic elution at constant } K_R)} \quad (9)$$

$$M = \frac{1}{2}\frac{1+HK_R}{GHJ(1+HK')} = \frac{1+HK_R}{1+HK'}\frac{B+1}{2B} \quad (10)$$

at $I = I_R$

$$J = \left|\frac{dK}{dI}\right| \quad (11)$$

$$\begin{aligned} L &= \frac{3.22M}{1+3.13M} \quad 0.25 \le M \le 12 \\ &= M^{0.5} \quad M < 0.25 \\ &= 1 \quad M > 12 \end{aligned} \quad (12)$$

Once the $A$ and $B$ values are determined by the $GH$–$I_R$ curve as explained above, $K_R$ can be calculated from Eq. (5) with the $I_R$ value for a given $GH$. Then, HETP (or $N$) in linear gradient elution (LGE) can be determined from the peak width $\sigma_{v,LGE}$ and the $I_R$ of the LGE curve by the following equation.

$$(HETP)_{LGE} = \frac{Z}{N_{LGE}} = \frac{1}{L^2}\frac{\sigma_{v,LGE}^2}{V_0^2}\frac{Z}{(1+HK_R)^2} \quad (13)$$

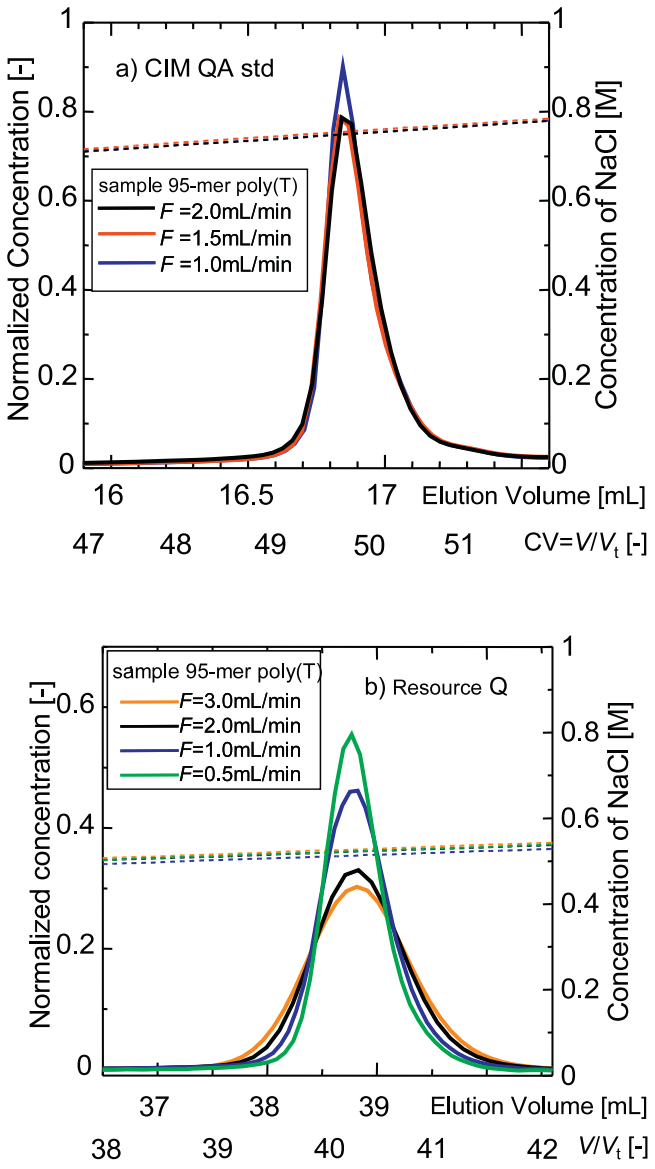


**Fig. 1.** Elution curves as a function of flow velocity in linear gradient elution. (a) Monolith chromatography: CIM-QA std ($Z$ = 3 mm, $d_c$ = 12 mm, $V_t$ = 0.34 mL). Sample: 95-mer poly (T), $V_g$ = 20 mL, $GH$ = 0.005 M, $I_0$ = 0.2 M. (b) Porous bead chromatography: Resource Q ($Z$ = 30 mm, $d_c$ = 6.4 mm, $\varepsilon$=0.39, $V_t$ = 0.965 mL). Sample: 95-mer poly (T), $V_g$ = 92 mL, $GH$ = 0.005 M, $I_0$ = 0.2 M.

here $K_R$ is the $K$ value at $I = I_R$. This method was already verified by Carta et al. [30].

### 3.3. van-Deemter HETP equation

A standard van-Deemter HETP equation is expressed as follows [10,23,31–35]

$$\mathrm{HETP} = A^0 + B^0/u + C^0u + D^0u \quad (14)$$

$A^0 = 2D_L/u$ is the axial dispersion term, which is a function of particle diameter $d_p$ for packed bed chromatography.

$B^0/u$ is the molecular diffusion term, which is not important for the present case.

$C^0u = (1/30)[HK/(1+HK)^2]\,(d_p^2/D_s)\,u$ is the stationary phase diffusion term, which governs the HETP for separation of large molecules.

$D^0u = (1/3)[HK/(1+HK)^2](Kd_p/k_f)u$ is the stagnant mass transfer term, which does not contribute to the HETP significantly for large molecule separations.

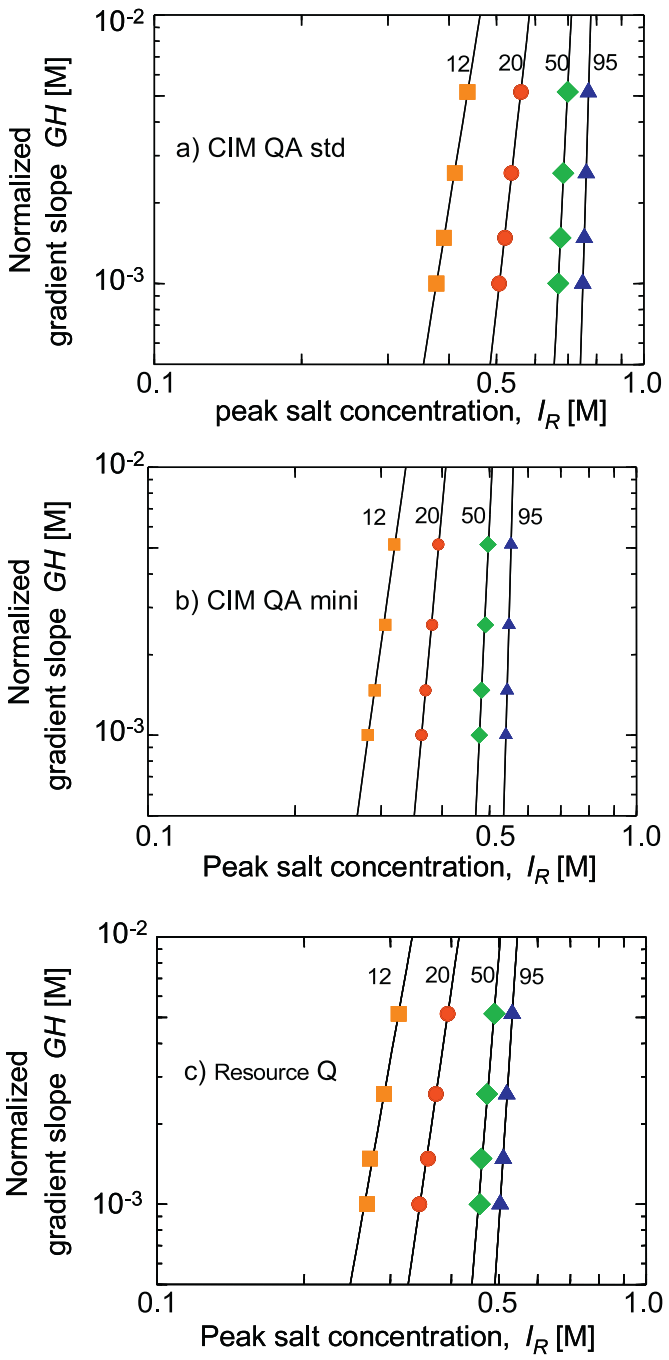


**Fig. 2.** $GH$–$I_R$ curves. The numbers in the figures 12, 20, 50 and 95 indicate 12-mer poly (T), 20-mer poly (T), 50-mer poly (T) and 95-mer poly (T), respectively. $I_0$ = 0.2 M, Flow rate $F$: 1.5 mL/min for CIM disk std, 0.28 mL/min for CIM disk mini, 2 mL/min for Resource Q

For chromatography of proteins and DNAs, Eq. (14) becomes

$$\mathrm{HETP} = A^0 + C^0u \quad (15)$$

For pure convection-controlling chromatography, $A^0$ is dominant in Eq. (14).

$$\mathrm{HETP} = A^0 \quad (16)$$

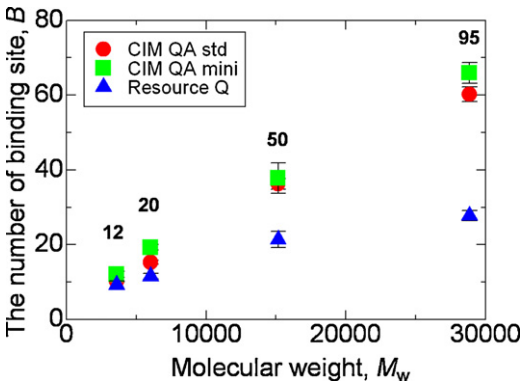


**Fig. 3.** Relationship between binding site $B$ and DNA size. The numbers in the figures 12, 20, 50 and 95 indicate 12-mer poly (T), 20-mer poly (T), 50-mer poly (T) and 95-mer poly (T), respectively. The $B$ values and the asymptotic standard error values are as follows: CIM QA std $B = 10.19 \pm 0.14$ (12T), $B = 15.31 \pm 0.55$ (20T), $B = 36.24 \pm 1.39$ (50T), $B = 60.20 \pm 1.96$ (95T), CIM QA mini $B = 12.04 \pm 0.76$ (12T), $B = 19.26 \pm 0.76$ (20T), $B = 37.83 \pm 4.06$ (50T), $B = 65.91 \pm 2.83$ (95T), Resource Q $B = 9.28 \pm 1.05$ (12T), $B = 11.54 \pm 0.75$ (20T), $B = 21.39 \pm 2.19$(50T), $B = 27.73 \pm 1.34$ (95T).

## 4. Results

### 4.1. Linear gradient elution curves

Typical linear gradient elution (LGE) curves as a function of flow velocity are shown in Fig. 1 for monolithic disk (CIM std) and porous bead chromatography (Resource Q). LGE curves in monolithic chromatography are not affected by the flow velocity whereas the peak width in porous bead chromatography become broader with increasing $u$ even though the particle diameter $d_p$ is small (15 μm). In all cases the peak retention volume $V_R$ was not affected by $u$. This flow-velocity dependent peak spreading was more significant compared with the data for smaller DNAs such as 12-mer and is due to the stationary phase (pore) diffusion resistance. The peak width for CIM std is quite narrow (ca. 0.5 mL), and small tailing and leading are observed. The tailing and leading might be mainly due to the spreading in the column housing [13].

### 4.2. GH–$I_R$ curves

In order to analyse the LGE peak width data by our method, it is needed to obtain GH–$I_R$ curves from LGE experiments. Fig. 2 shows GH–$I_R$ curves for the three columns. As already reported in our previous studies [20,22], the slope becomes steeper and shifts to larger $I_R$ values with increasing DNA size. This means that the binding site $B$ value increases and higher salt concentration is needed for elution when DNA becomes large.

The binding site $B$ (effective charge) values obtained from these GH–$I_R$ curves are shown in Fig. 3. The $B$ values for CIM std and CIM mini are similar irrespective of DNA size. Compared with the data for the CIM disks the $B$ value for Resource Q is slightly lower for 12- and 20-mer DNAs, and considerably lower for 95-mer DNA. The $B$ values were determined by the least square fitting method. The correlation coefficient was quite high ($r^2 > 0.9$). However, for such high $B$ values as $B > 40$ the exact value does not have a physical meaning. It simply implies that a very large number of binding sites is responsible for the interaction.

### 4.3. Peak width as a function of distribution coefficient at the peak retention volume

As explained previously, a simple method for measuring HETP is not applicable to LGE curve as the retention volume $V_R$ is not directly connected with the constant distribution coefficient like isocratic elution.

Therefore, we correlated the peak width with the distribution coefficient at the retention volume, $K_R$. Our previous study has shown a good correlation between the peak width and $K_R$ [20]. However, in this study in order to understand the zone spreading

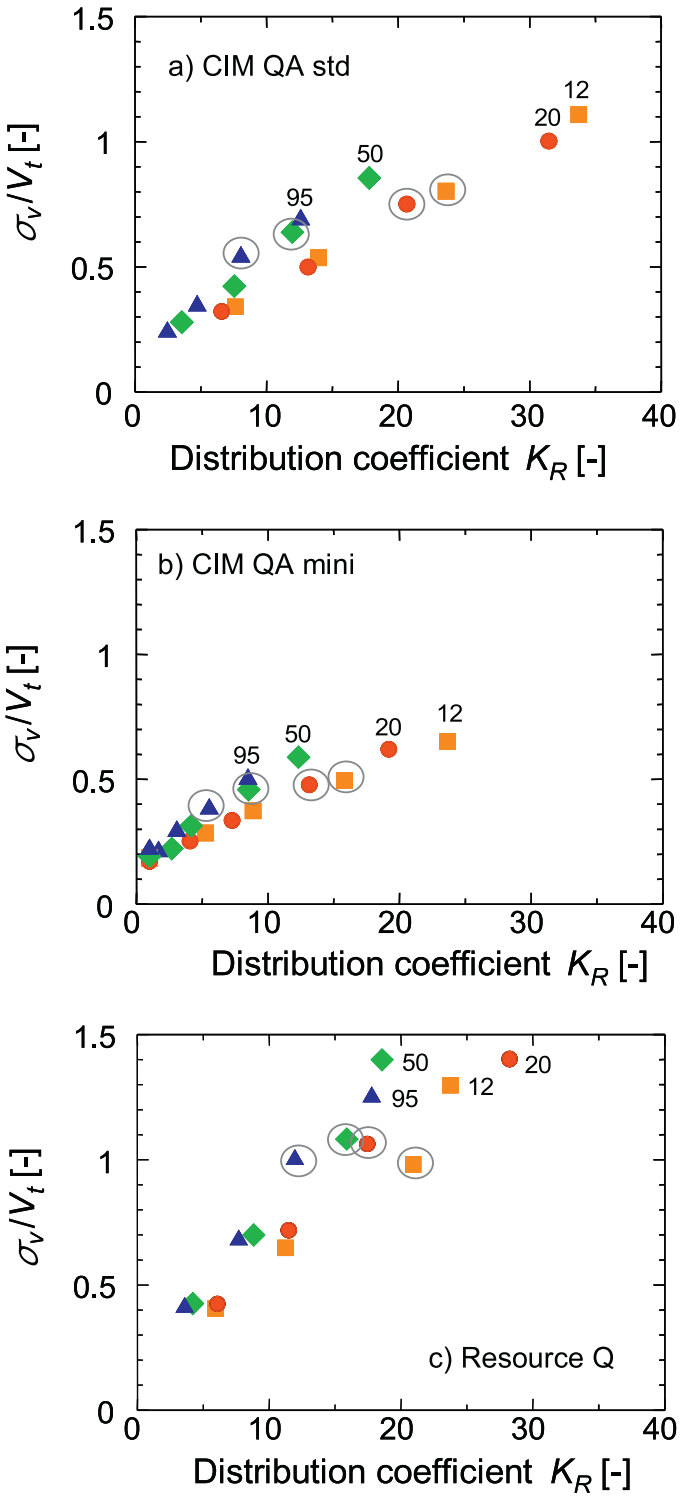


**Fig. 4.** Peak width normalized with the bed volume as a function of the distribution coefficient at the peak $K_R$. The numbers in the figures 12, 20, 50 and 95 indicate 12-mer poly (T), 20-mer poly (T), 50-mer poly (T) and 95-mer poly (T), respectively. The data encompassed by circles are for the same gradient slope. $I_0 = 0.2$ M, Flow rate $F$: 1.5 mL/min for CIM disk std, 0.28 mL/min for CIM disk mini, 2 mL/min for Resource Q.

mechanism quantitatively, the peak width normalized with the bed volume $V_t$ was correlated to $K_R$ as shown in Fig. 4. For Resource Q, although the peak width changes with the flow velocity as shown in Fig. 1 the data at $F = 2.0\,cm^3/min$ (the residence time ca. 30 s) are shown. Good correlation is found for the three chromatography columns. However, the relative peak width values for the monolith disks are much smaller than those for Resource Q especially for large DNAs. For monolith chromatography the relative peak width values for DNAs of different sizes are similar whereas the values for large DNAs are larger for Resource Q.

As explained in detail in our previous study, for monolith chromatography the relative peak width becomes narrower with increasing DNA size in LGE with the same slope. This can be easily confirmed in Fig. 4. For Resource Q porous bead chromatography this effect is not valid due to the pore diffusion resistance of large DNAs.

### 4.4. HETP from linear gradient elution curves

In order to understand the peak width data more precisely apparent HETP values were calculated according to our method [21], and plotted against the $K_R$ values (Fig. 5). HETP values are almost constant (ca. 0.0025 cm) when $K_R > 5$ for CIM std. As for CIM mini similar HETP values were obtained when $K_R > 15$. However, a significant increase of HETP is observed when $K_R$ decreases from 10 to 1. This is mainly due to the contribution of extra column broadening as the actual peak width becomes very small as shown in Fig. 4. Constant HETP values mean that the peak width increases with the retention volume, which is related to the distribution coefficient (see. Eq. (13)). We did not subtract the zone spreading due to the extra-column as it is difficult to assess the realistic value. The peak is quite sharp for steep gradient slopes where $K_R$ values are low (<2). A typical baseline peak width for the 0.34 mL disk was ca. 0.2 mL at $K_R = 1$ (see Fig. 4). When the gradient slope is shallow, it was ca. 1 mL or larger. For these shallow gradient slope data HETP values were precisely calculated. We did isocratic elution experiments for relatively large $K_R$ values. The data are shown in Fig. 5a, where both the data from LGE and those from isocratic elution are similar. The HETP values from both isocratic and linear gradient elution experiments for $K_R > 5$ are constant since mass transfer does not affect the peak spreading and the contribution due to the extra-column broadening is not significant.

As HETP is a function of flow velocity for Resource Q column data, it is not easy to understand the data shown in Fig. 5. However, as is clear from the figure HETP values are much higher than those for monolithic chromatography.

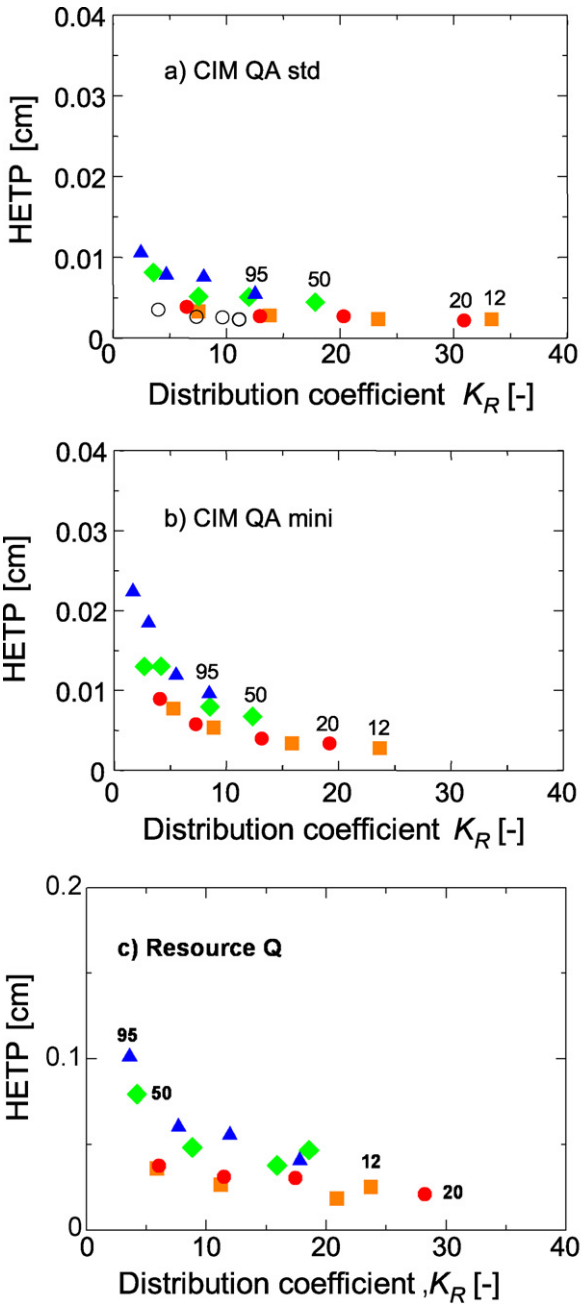


**Fig. 5.** HETP determined from linear gradient elution curves as a function of the distribution coefficient at the peak $K_R$. The numbers in the figures 12, 20, 50 and 95 indicate 12-mer poly (T), 20-mer poly (T), 50-mer poly (T) and 95-mer poly (T), respectively. $I_0 = 0.2$ M, Flow rate $F$: 1.5 mL/min for CIM disk std, 0.28 mL/min for CIM disk mini, 2 mL/min for Resource Q. The open circle symbols are data by isocratic elution experiments for 20-mer poly (T).

## 5. Discussion

There are many different approaches for understanding the zone spreading in convection-aided (perfusion) or convection-controlling chromatography [1–10,16–18,33]. Expanded or modified van-Deemter equations for convection-aided chromatography are based on the assumption that the rate model considering the axial dispersion and the stationary phase diffusion can describe the zone spreading in convection-aided chromatography when additional parameters for the perfusion effect are incorporated into the model [1,3–7,10,33]. Therefore, the contribution of axial dispersion and stationary phase diffusion to the total zone spreading is significant even when the perfusion effect dominates (HETP or peak width remains constant at high flow velocities). Therefore, it is not possible to obtain sharp elution peaks at high flow velocities for process-scale chromatography due to their large particle size.

On the other hand, zone spreading in convection-controlling chromatography like monolith chromatography is not affected by stationary phase diffusion even at low flow velocities. HETP does not change with flow-velocity and is a function of axial dispersion in the bed. The axial dispersion mechanism is rather difficult to understand. Flow-channel irregularities due to stacked membranes and/or mal-flow distribution might cause the axial dispersion [8,9]. More detailed and rigorous models considering a bed as a bundle of capillaries have been proposed [36]. However, for monolith chromatography as the bed is continuous and is regarded as a pseudo-packed bed of non-porous beads. It is reasonable to assume that the axial dispersion is similar to that for the packed bed. Frey et al. [8] has investigated the axial dispersion in stacked membrane chromatography along with the data by

Briefs and Kula [37]. The normalized HETP (=HETP/membrane pore diameter) ranges between 100 and 250. Our data shows that HETP is 0.003–0.005 cm, which corresponds to the normalized HETP (=HETP/monolith pore diameter) 20–33 assuming that the pore diameter is ca 1.5 μm (the total number of plates for the 3 mm disk is ca. 100). These data clearly indicate much smaller peak spreading in monolithic chromatography compared with stacked membrane chromatography.

The normalized HETP with the pore diameter was reported to be around 20 for a silica monolith rod [15]. Similar data were reported also for analytical scale silica monolith chromatography [17,18]. The continuous phase structure of monolith rather than discontinuous stacked membrane structure results in much smaller dispersion in the bed. The HETP values determined from linear gradient elution (LGE) curves are more reproducible as the (self) zone sharpening effect can improve the distorted zone initially formed near the column inlet. The sample volume also does not affect the peak spreading due to the tight (strong) binding at the initial mobile phase conditions. The HETP values for relatively large $K_R$ values by isocratic elution experiments were similar to those obtained by LGE experiments as shown in Fig. 5. It should be noted here that the peak width at 0.368 × peak height, was measured in order to determine the peak variance. We did not employ the moment method as it is quite sensitive to a small amount of tailing and leading for such sharp peaks [23,31,33]. When the sample has a micro-heterogeneity and the column performance is high, the peak shape does not become symmetrical and may have leading and/or tailing. Aggregation might cause such leading and tailings although all samples were thermally pretreated prior to use. When HETP is constant the peak width normalized with the bed volume should increase with the corrected elution volume according to Eq. (13). This is clearly shown in Fig. 4. However, for small $K_R$ values both the peak with and the retention volume become smaller. Therefore, even a small contribution due to the extra-column broadening affects the HETP values. This is the reason why HETP values for small $K_R$ values are larger.

Currently most membrane-based chromatography is aimed for removal of contaminants [11,12]. Therefore, the desorption or elution performance is not considered important. When monolith chromatography is employed for purification of bioparticles such as pDNA and vaccines, it is important to obtain sharp elution peaks [38]. Stepwise elution chromatography can be also analysed based on our model [23,24]. As explained in our previous studies [23], stepwise elution under complete desorption conditions can be regarded as LGE with a very sharp gradient slope (type I elution). The normalized peak width of type I stepwise elution in monolith chromatography (CIM std) was ca. 0.13–0.15, which agrees well with the value shown in Fig. 4 (the value at $K_R = 1$).

## Acknowledgements

This work was partly supported by a Grant-in Aid for scientific research (B2, No. 21360382) from the Ministry of Education, Science, Sports and Culture, Japan, and also by a project "Development of New Functional Antibody Technologies" of The New Energy and Industrial Technology Development Organization (NEDO), Japan

## References

[1] N.B. Afeyan, N.F. Gordon, I. Mazsaroff, L. Varady, S.P. Fulton, Y.B. Yang, F.E. Regnier, J. Chromatogr. 519 (1990) 1.
[2] A.I. Liapis, M.A. McCoy, J. Chromatogr. 599 (1992) 87.
[3] D.D. Frey, E. Schweinheim, Cs. Horváth, Biotechnol. Prog. 9 (1993) 273.
[4] D. Farnan, D.D. Frey, Cs. Horváth, Biotechnol. Prog. 13 (1997) 429.
[5] G. Carta, A.E. Rodriguez, Chem. Eng. Sci. 48 (1993) 3927.
[6] A.E. Rodriguez, J.M. Loureiro, C. Chenou, M. Rendules de la Vega, J. Chromatogr. B 664 (1995) 233.
[7] G. Carta, Chem. Eng. Sci. 50 (1995) 887.
[8] D.D. Frey, R. van der Water, B. Zhang, J. Chromatogr. 603 (1992) 43.
[9] S.-Y. Suen, M.R. Etzel, Chem. Eng. Sci. 47 (1992) 1355–1364.
[10] M. Ladisch, Bioseparations Engineering: Principles, Practice, and Economics, Wiley, New York, 2001.
[11] U. Gottschalk, Biotechnol. Prog. 24 (2008) 496.
[12] U. Gottschalk, Adv. Biochem. Eng. Biotech. 115 (2010) 171.
[13] A. Jungbauer, R. Hahn, J. Chromatogr. A 1184 (2008) 62.
[14] N.L. Krajnc, F. Smrekar, V. Smrekar, A. Štrancar, A. Podgornik, Monolithic Macroporous Polymers as Chromatographic Matrices, V: Macroporous Polymers: Production Properties and Biotechnological/Biomedical Applications, CRC Press, Boca Raton, 2009, pp. 291–334.
[15] M. Zabka, M. Minceva, A.E. Rodrigues, Chem. Eng. Process.: Process Intensification 45 (2006) 150.
[16] A. Podgornik, M. Barut, S. Jaksa, J. Jancar, A. Strancar, J. Liq. Chromatogr. Related Technol. 25 (2002) 3099.
[17] K. Miyabe, G. Guiochon, J. Phys. Chem. A 106 (2002) 8898.
[18] K. Miyabe, G. Guiochon, J. Sep. Sci. 27 (2004) 853.
[19] S. Yamamoto, A. Kita, Food Bioproducts Process. 84 (2006) 72.
[20] S. Yamamoto, N. Yoshimoto, Y. Nishizumi, J. Chromatogr. A 1216 (2009) 2612.
[21] S. Yamamoto, Biotechnol. Bioeng. 48 (1995) 444.
[22] S. Yamamoto, M. Nakamura, C. Tarmann, A. Jungbauer, J. Chromatogr. A 1144 (2007) 155.
[23] S. Yamamoto, K. Nakanishi, R. Matsuno, Ion-Exchange Chromatography of Proteins, Marcel Dekker, New York, 1988.
[24] S. Yamamoto, Chem. Eng. Technol. 28 (2005) 1387.
[25] N.K. Boardman, S.M. Partridge, Biochem. J. 59 (1955) 543.
[26] F.E. Regnier, I. Mazsaroff, Biotechnol. Prog. 3 (1987) 22.
[27] S.R. Gallant, S. Vunnum, S.M. Cramer, J. Chromatogr. A 725 (1996) 295.
[28] S. Ghose, S.M. Cramer, J. Chromatogr. A 928 (2001) 1323.
[29] A. Velayudhan, C. Horvath, J. Chromatogr. A 443 (1988) 13.
[30] L.R. Snyder, High Perform Liq. Chromatogr. 1 (1980) 207.
[31] M. D. LeVan, G. Carta, C.M. Yon, D. W. (ed.), Perry's Chemical Engineers' Handbook (7th ed.), McGraw-Hill, New York, 1997.
[32] G. Carta, A.R. Ubiera, T.M. Pabst, Chem. Eng. Technol. 28 (2005) 1252.
[33] G. Carta, A. Jungbauer, Protein Chromatography, Wiley-VCH, Weinheim, 2010.
[34] R.G. Harrison, P. Todd, S.R. Rudge, D.P. Petrides, Bioseparations Science and Engineering, Oxford University Press, New York, 2003, Chapter 7.
[35] G. Guiochon, S.G. Sirazi, A.M. Katti, Fundamentals of Preparative and Nonlinear Chromatography, Academic Press, Boston, 1994.
[36] J.J. Meyers, A.I. Liapis, J. Chromatogr. A 852 (1999) 3–23.
[37] K.-G. Briefs, M.-R. Kula, Chem. Eng. Sci. 47 (1992) 141.
[38] J. Urthaler, R. Schlegl, A. Podgornik, A. Strancar, A. Jungbauer, R. Necina, J. Chromatogr. A1065 (2005) 93.